Available online at www.sciencedirect.com
ScienceDirect
Journal of Sound and Vibration 318 (2008) 93–108
JOURNAL OF SOUND AND VIBRATION
www.elsevier.com/locate/jsvi

Tuneable vibration absorber design to suppress vibrations: An application in boring manufacturing process

H. Moradi[a], F. Bakhtiari-Nejad[b,*], M.R. Movahhedy[a]

[a]*School of Mechanical Engineering, Sharif University of Technology, Tehran, Iran*
[b]*Amirkabir University of Technology, Tehran, Iran*

Received 17 December 2007; received in revised form 2 April 2008; accepted 2 April 2008
Handling Editor: C.L. Morfey
Available online 16 May 2008

Abstract

Dynamic vibration absorbers are used to reduce the undesirable vibrations in many applications such as electrical transmission lines, helicopters, gas turbines, engines, bridges, etc. Tuneable vibration absorbers (TVA) are also used as semi-active controllers. In this paper, the application of a TVA for suppression of chatter vibrations in the boring manufacturing process is presented. The boring bar is modeled as a cantilever Euler–Bernoulli beam and the TVA is composed of mass, spring and dashpot elements. In addition, the effect of spring mass is considered in this analysis. After formulation of the problem, the optimum specifications of the absorber such as spring stiffness, absorber mass and its position are determined using an algorithm based on the mode summation method. The analog-simulated block diagram of the system is developed and the effects of various excitations such as step, ramp, etc. on the absorbed system are simulated. In addition, chatter stability is analyzed in dominant modes of boring bar. Results show that at higher modes, larger critical widths of cut and consequently more material removal rate (MRR) can be achieved. In the case of self-excited vibration, which is associated with a delay differential equation, the optimum absorber suppresses the chatter and increases the limit of stability.

1. Introduction

Vibration is an undesirable phenomenon in machining processes because it results in the reduction of material removal rate (MRR), poor surface finish and increased tool wear. Two major types of vibration occurring in machining are forced vibrations and self-excited vibrations. The unbalance of rotating members, servo instability, or force on a multi-tooth cutter may result in forced vibration. The cutting tool oscillates at the frequency of the cutting force. When this frequency is close to a natural frequency of the tool, large-amplitude vibrations due to resonance occur.

Self-excited vibration or chatter is the most important type of vibration in machining processes [1]. Two mechanisms known as regeneration [2] and mode coupling [3] are the major reasons for machine–tool chatter.

*Corresponding author. Tel.: +98 21 64543417; fax: +98 21 66419736.
E-mail address: baktiari@aut.ac.ir (F. Bakhtiari-Nejad).

0022-460X/$ - see front matter © 2008 Elsevier Ltd. All rights reserved.
doi:10.1016/j.jsv.2008.04.001

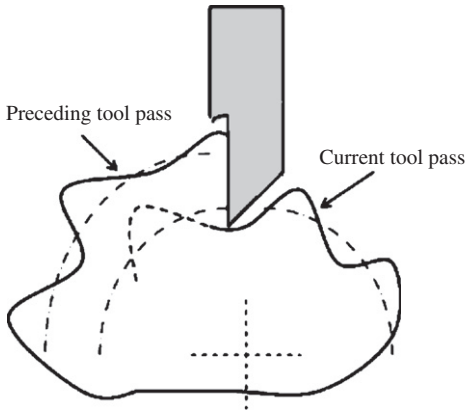

Fig. 1. Instability caused by regeneration.

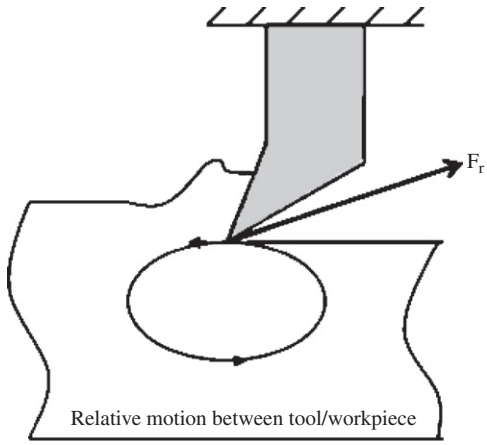

Fig. 2. Instability caused by mode coupling.

The former, as shown in Fig. 1, is due to the interaction of the cutting force and the workpiece surface undulations produced by preceding tool passes. Regenerative chatter occurs when cuts overlap and the cut produced at time t leaves small waves in the material that are regenerated during each subsequent pass of the tool. The regenerative type is found to be the most detrimental to the production rate in most machining processes. If regenerative vibrations become large enough that the tool does not contact the workpiece, another type of chatter known as multiple-regenerative chatter occurs.

Mode coupling is produced by relative vibration between the tool and the workpiece that occur simultaneously in two different directions in the plane of cut. In fact, mode coupling usually occurs when there is no interaction between the vibration of the system and undulated surface of the workpiece. In this case, the tool traces out an elliptic path that varies the depth of cut in such a way as to bolster the coupled modes of vibrations (as shown in Fig. 2). The amplitude of self-excited vibration increases until some nonlinearities in the machining process limit this amplitude [4]. Other mechanisms have been presented. For example, in one mechanism, the cutting forces depend on velocity such that they induce a negative damping in the turning process [5]. In fact, this mechanism is a frictional effect and has similar characteristics to that of the Rayleigh oscillator [6]. In addition, some works have been done in which the nonlinear equation, with delay time, is associated with a nonlinear structure of stiffness and nonlinear equations of high order for depth of cut in cutting force expression [7–9]. Self-excited frequency is usually close to a natural frequency of the cutting system.

Many works have been carried out to suppress regenerative chatter using both passive [10–12] and active [13–15] vibration absorbers. Using impact and particle dampers [16,17] is another approach for tooling with embedded absorbers. But in all of these works, a single-degree-of-freedom model (sdof) has been used to model the boring bar in the boring process and the cutting tool or workpiece in the turning process. In addition, in the previous works the designed absorber has a fixed position while in this paper the optimum position of the absorber is determined. Proper spindle-speed selection [18] and spindle-speed variation [19,20] are other strategies developed in conjunction with the stability lobes diagrams. Also active [21], optimal [22] and adaptive [23] controllers are used to suppress regenerative chatter. These approaches are employed for various machining processes such as turning, milling and boring processes. Chatter is particularly critical for the boring process, because the common long tool overhang in this process makes it very susceptible to chatter, and the requirement on surface quality is usually more stringent.

In most of the works presented for chatter suppression in the boring process, the boring tool system is modeled using a sdof. Consequently, only a single mode of vibration is predicted from this model. This assumption may not be sufficiently accurate, because the boring bar is a continuous system and contains an infinite number of vibration modes. So, when the control procedure is developed to suppress only the dominating mode, the rest of the structural modes may be excited, resulting in a spill-over problem [21]. In addition, the process of the absorber design relies on the fact that the model parameters such as mass, stiffness and damping are accurate. But both the nature of the boring process as a dynamic system and the existence of movable elements of the machine–tool and the workpiece make it difficult to obtain accurate results from an sdof system.

In this paper, a dynamic system containing a TVA applied on an Euler–Bernoulli beam is considered. The formulation is derived for a TVA composed of mass, spring and damper elements. Then the formulation is developed more and the effect of spring mass is considered too [24]. The designed TVA is applied for suppression of self-excited vibrations in the boring manufacturing process in which the boring bar is modeled as a cantilever Euler–Bernoulli beam. The optimum values of the absorber parameters such as spring stiffness, absorber mass and its position are determined using an algorithm based on the mode summation method.

2. Horizontal boring machines

Horizontal boring machines are very versatile and thus particularly useful in machining large parts. The basic components of these machines are as follows [25]:

- A rotating spindle that can be fed horizontally (tool rotates).
- A table that can be moved and fed in two directions in a horizontal plane.
- A headstock that can be moved vertically.
- An outboard bearing support for a long boring bar.

The spindle can embed boring bars, drills and milling cutters. As the spindle speed varies in a wide range, heavy bearings are incorporated to absorb thrust in all directions. Drilling and boring can be performed without moving the table because the spindle can be fed longitudinally.

A rotating single-point tool is usually used in the boring process. Tools can be inserted either in a sub-type bar, held only in the spindle, or in a boring bar as shown in Fig. 3. Horizontal boring machines are used primarily for boring holes less than 12 in in diameter, long holes, or for a series of in-line holes [25].

3. Modeling of a boring bar with a vibration absorber

Structures made of several beams are common in engineering fields. Each beam is constituted by an infinite number of degrees of freedom, and the mode summation method is used to model it as a system consisting of a finite number of, more significant, degrees of freedom. Constraints such as additional supports on the structure alter the normal modes of the system. For forced vibration of a one-dimensional structure, a force per unit length $f(x,t)$ at any location of x is considered. If normal modes of the structure $\phi_i(x)$ are known, its

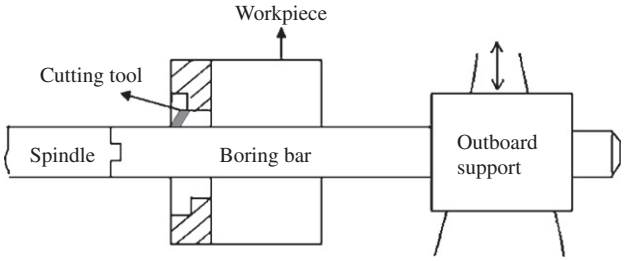

Fig. 3. Horizontal boring machine with a long boring bar.

deflection at any point x can be expressed as

$$y(x,t)=\sum_i q_i(t)\phi_i(x) \tag{1}$$

where the generalized coordinate $q_i(t)$ must satisfy the following equation [26]:

$$\ddot{q}_i(t)+2\zeta_i\omega_i\dot{q}_i(t)+\omega_i^2 q_i(t)=\frac{1}{m_i}\int f(x,t)\phi_i(x)\,\mathrm{d}x \tag{2}$$

and the generalized mass m_i is defined as

$$m_i=\int \rho\phi_i^2(x)\,\mathrm{d}x \tag{3}$$

The damping ratio ζ_i is a small positive number with common values of $\zeta_i\leqslant 0.05$ for slightly damped structures and ρ is the mass per unit length of the beam. For a cantilever Euler–Bernoulli beam, the eigenvector at any mode is given as

$$\begin{aligned}&\phi_i(x)=A_i[\cosh\lambda_i x-\cos\lambda_i x-\mu_i(\sinh\lambda_i x-\sin\lambda_i x)]\\&\mu_i=\frac{\cosh\lambda_i+\cos\lambda_i}{\sinh\lambda_i+\sin\lambda_i}\end{aligned} \tag{4}$$

and the natural frequencies of a cantilever beam are defined as

$$\omega_i=\left(\frac{\lambda_i}{l}\right)^2\sqrt{\frac{EI}{\rho}} \tag{5}$$

where EI is flexural rigidity, l is the beam length. After applying the boundary conditions for a cantilever beam, λ_i's can be determined from the following characteristic equation:

$$\cos\lambda_i l\,\cosh\lambda_i l+1=0$$

λ_i are constants taking the following values that for the first three natural frequencies are:

$$\lambda_1=1.87,\quad \lambda_2=4.69,\quad \lambda_3=7.85$$

Normal modes $\phi_i(x)$ are orthogonal functions that satisfy the following relationship:

$$A_i^2\int \phi_i(x)\phi_i(x)=1 \tag{6}$$

Substituting Eq. (4) in Eq. (6) results in $A_i=1$. If instead of distributed load $f(x,t)$ a concentrated force $F(a,t)$ is applied at some point $x=a$ along the beam length, Eq. (2) can be written as

$$\ddot{q}_i(t)+2\zeta_i\omega_i\dot{q}_i(t)+\omega_i^2 q_i(t)=\frac{1}{m_i}F(a,t)\phi_i(a) \tag{7}$$

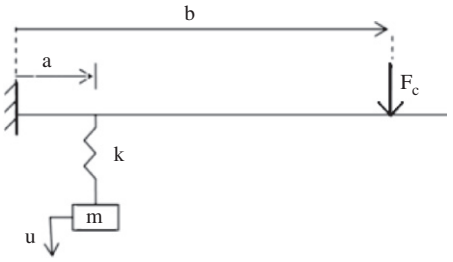

Fig. 4. Vibration system under cutting force and absorber.

In the presence of regenerative chatter, the cutting force is proportional to the chip area and is represented as [1]

$$F_c = k_c w_c[h_0 + y(x, t-T) - y(x,t)], \quad T = 60/N \tag{8}$$

where k_c is the cutting coefficient determined by tool geometry and workpiece material, w_c is the width of cut, h_0 is the nominal value of the chip thickness, $y(x,t)$ is defined by Eq. (1), T is the time period (delay) between the current time and previous time the tool has passed the point in consideration and N is the spindle rotational speed (rpm). Considering the effect of regenerative chatter, Eq. (7) is modified to

$$\ddot{q}_i(t) + 2\zeta_i\omega_i\dot{q}_i(t) + \omega_i^2 q_i(t) + \delta\sum_j (q_j(t) - q_j(t-T))\phi_j(a) = \frac{1}{m_i}F(a,t)\phi_i(a) \tag{9}$$

where $\delta = k_c w_c/m_i$ and $F(a,t) = k_c w_c h_0$, which does not change with time and is the constant part of the cutting force described in Eq. (8).

3.1. Mass–spring absorber

The boring bar is modeled as a cantilever beam as shown in Fig. 4. A vibration absorber consisting of a lumped mass attached to a spring is applied to the beam at a distance $x = a$ from the clamped support and the cutting tool is located at position $x = b$ (not necessarily at the free end). The deflection of the beam at the absorber location is $y(a,t)$ and the displacement of the mass of the absorber is denoted as u. Then, Eq. (9) is rewritten as

$$\ddot{q}_i(t) + \omega_i^2 q_i(t) + \delta\sum_j (q_j(t) - q_j(t-T))\phi_j(b) = \frac{1}{m_i}\{-k[y(a,t) - u(t)]\phi_i(a) + k_c w_c h_0 \phi_i(b)\} \tag{10}$$

Since the constant part of cutting force, $k_c w_c h_0$, is too small with respect to other parts of Eq. (10), this part can be eliminated. In fact, the self-excited vibration is caused chiefly by the time-variable part of the cutting force, $\delta\sum q_j(t) - q_j(t-T)$ (this fact can be easily verified by the results of simulation in SIMULINK Toolbox of MATLAB). Under oscillatory conditions and by neglecting the constant value of Eq. (10), the normal modes and the displacement of the absorber can be written in the exponential form as

$$q_i = \overline{q}_i e^{j\omega t}, \quad u = \overline{u} e^{j\omega t} \tag{11}$$

Using these exponential forms and substituting Eq. (1) in Eq. (10) yields

$$\overline{q}_i(t)(\omega_i^2 - \omega^2) + \delta\sum_j (\overline{q}_j(t) - \overline{q}_j(t-T))\phi_j(b) + \alpha\phi_i(a_1)\sum_j \phi_j(a_1)\overline{q}_j(t) - \alpha\phi_i(a_1)\overline{u}(t) = 0 \tag{12}$$

where $\alpha = k/m_i$. The vibration equation for the absorber is written as

$$m\ddot{u}(t) + k[u(t) - y(a,t)] = 0 \tag{13}$$

Similarly, using the exponential form of Eq. (11) in Eq. (13) yields

$$\overline{u}[\beta - \omega^2] - \beta\sum_j \phi_j(a)\overline{q}_j = 0 \tag{14}$$

where $\beta = k/m$. The coupled system of Eqs. (12) and (14) is the vibration equations for the combined dynamic system. In the presence of regenerative chatter, this set of equations can be solved using a MATLAB code or SIMULINK Toolbox of MATLAB software. For the case of forced vibrations, these equations can be written in the matrix form as $\mathbf{AQ} = \mathbf{0}$. **A** is a full-rank matrix of order $(n+1)$ with elements that are the coefficients of $\overline{q}_i$ and $\overline{u}$, **Q** is a vector whose elements are $\overline{q}_i$ and $\overline{u}$. If the determinant of **A** is set to zero, the $(n+1)$ natural frequencies of the whole system including the beam and the absorber can be obtained. To obtain the generalized coordinate $\overline{q}_i$ and the amplitude of the absorber mass displacement $\overline{u}$, Eqs. (12) and (14), which are $(n+1)$ coupled equations, must be solved simultaneously. It should be mentioned that in the closed-form equation $\mathbf{AQ} = \mathbf{0}$ all $\overline{q}_i$ cannot be zero because this is a coupled system of delayed equations including $\overline{q}_i(t-T)$ terms.

3.2. Mass–spring–damper absorber

The TVA composed of the mass and the spring is sufficient for the purpose of this paper: chatter suppression in the boring manufacturing process. So, it is not necessary to apply the TVA including damping. However, the TVA including damping may be useful in other applications with more precise assumptions. So the following formulation has been developed and presented for future works.

An absorber made of a mass, a spring and a damper is considered as shown in Fig. 5. To make the modeling more general, it is assumed that the spring and the damper are applied at two different points as shown in Fig. 5. The distance between the spring and the clamped support (a_1) is selected as a design parameter. Referring to Fig. 5, Eqs. (10) and (13) are rewritten as

$$\ddot{q}_i(t) + 2\zeta_i\omega_i\dot{q}_i(t) + \omega_i^2 q_i(t) + \delta\sum_j (q_j(t) - q_j(t-T))\phi_j(b) = \frac{1}{m_i}\{-k[y(a_1,t) - u(t)]\phi_i(a_1) - c[\dot{y}(a_2,t) - \dot{u}(t)]\phi_i(a_2) + k_c w_c h_0 \phi_i(b)\} \tag{15}$$

$$m\ddot{u}(t) + c[\dot{u}(t) - \dot{y}(a_2,t)] + k[u(t) - y(a_1,t)] = 0 \tag{16}$$

Using the steps similar to those in the previous section, it can be shown that the vibration equations of this system are expressed as

$$\overline{q}_i(t)[\omega_i^2 - \omega^2] + \mathrm{j}[2\zeta_i\omega_i\overline{q}_i(t) + \xi\omega\phi_i(a_2)\sum_j \phi_j(a_2)\overline{q}_j(t)] + \delta\sum_j(\overline{q}_j(t) - \overline{q}_j(t-T))\phi_j(b) + \alpha\phi_i(a_1)\sum_j \phi_j(a_1)\overline{q}_j(t) - \overline{u}(t)[\alpha\phi_i(a_1) + \mathrm{j}\xi\omega\phi_i(a_2)] = \gamma\phi_i(b) \tag{17}$$

$$\beta\sum_j \phi_j(a_1)\overline{q}_j + \mathrm{j}\eta\omega\sum_j \phi_j(a_2)\overline{q}_j + \overline{u}[\omega^2 - \beta - \mathrm{j}\eta\omega] = 0 \tag{18}$$

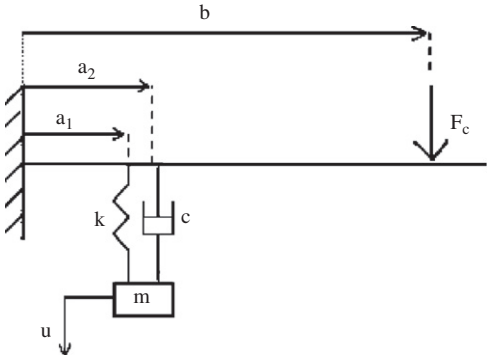

Fig. 5. Vibration system under the cutting force and absorber.

where $\xi = c/m_i$ and $\eta = c/m$. General coordinates $\overline{q}_i$ and the absorber mass displacement $\overline{u}$ are found by solving Eqs. (17) and (18); substituting the general coordinates $\overline{q}_i$ into Eq. (1) yields the beam deflection at any point.

3.3. Spring mass effect on the formulation of the problem

In the analysis given in the previous sections, the spring mass was neglected. In many practical cases, neglecting this mass has an important effect on the dynamic analysis of the system. To prevent from busy equations and only studying the effect of spring mass, the analysis is done for the dynamic model without chattering (forced vibration is considered). Velocity of the spring at a connected point to the beam is considered as $\dot{y}(a,t)$ and at the connected end to the mass is $\dot{u}$ and change is assumed linearly as shown in Fig. 6. An element with the length of $\mathrm{d}\lambda$ at a distance of λ from the top of the spring is considered. From Fig. 6 the velocity of this element can be written as $V(\lambda) = \dot{y}(a,t) + (\dot{u} - \dot{y}(a,t))(\lambda/L)$, in which $\dot{y}(a,t) = \sum \phi_i(a)\dot{q}_i(t)$ and L is the free length of the spring and $m_s = \rho_s L$ denotes the spring mass and ρ_s is the mass per length of the spring. So potential and kinetic energies for the system are written as

$$T = \frac{1}{2}\sum_i m_i\dot{q}_i^2 + \frac{1}{2}m\dot{u}^2 + \frac{1}{2}\int_0^l (\rho\,\mathrm{d}\lambda)\left[\sum_i \phi_i(a)\dot{q}_i^2 + \frac{\dot{u} - \sum_i \phi_i(a)\dot{q}_i}{L}\lambda\right]^2 \tag{19}$$

$$U = \frac{1}{2}k\left(\sum_i \phi_i(a)q_i - u\right)^2 + \frac{1}{2}\sum_i \omega_i^2 m_i q_i^2 \tag{20}$$

Generalized force is $Q_i = F_0\phi_i(b)\sin\omega t$. Substituting Eqs. (19) and (20) into the Lagrange's equation [23], the vibration equations of the whole system are expressed by

$$\begin{cases} \overline{q}_i(\omega_i^2 - \omega^2) + (\alpha - \underline{\alpha_1\omega^2})\phi_i(a)\sum_j \phi_j(a)\overline{q}_j - (\alpha + \underline{\alpha_2\omega^2})\phi_i(a)\overline{u} = \gamma'\phi_i(b) & \text{(I)} \\ (\omega^2 - \beta)\overline{u} + (\beta' + \underline{\alpha_3\omega^2})\sum_j \phi_j(a)\overline{q}_j = 0 & \text{(II)} \end{cases} \tag{21}$$

where

$$\alpha = k/m_i, \quad \beta = k/m, \quad \beta' = \frac{k}{m + m_s/3}, \quad \gamma' = \frac{F_0}{m_i}, \quad \alpha_1 = \frac{m_s}{3m_i}, \quad \alpha_2 = \frac{m_s}{6m_i}, \quad \alpha_3 = \frac{m_s/6}{m + m_s/3} \tag{22}$$

In Eq. (21), the expressions specified with a dashed line, without considering the effect of regenerative chatter, are added with respect to Eqs. (12) and (14) [21], $\overline{q}_i$ and $\overline{u}$ are found by solving Eq. (21). Using Eq. (1), the deflection of the beam will be achieved. It can be shown that for beams with high natural frequencies, the

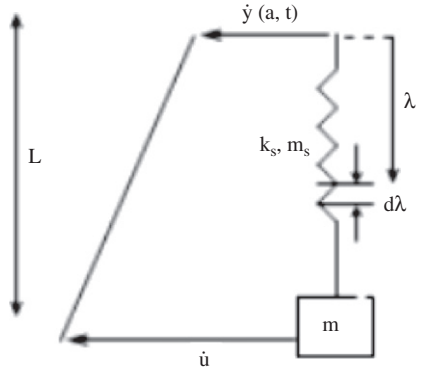

Fig. 6. Variation of the absorber spring velocity.

values of α_i, $i = 1,2,3$ are so small that the natural frequencies of the absorbed beam remain almost constant. Similarly, for the system with an absorber made of mass, spring and damper, Eq. (21) is changed to

$$\begin{cases} \overline{q}_i(\omega_i^2 - \omega^2) + (\alpha - \alpha_1\omega^2)\phi_i(a_1)\sum_j \phi_j(a_1)\overline{q}_j + \mathrm{j}\xi\omega\phi_i(a_2)\sum_j \phi_j(a_2)\overline{q}_j - (\alpha + \alpha_2\omega^2)\phi_i(a_1)\overline{u} \\ \quad -\mathrm{j}\xi\omega\phi_i(a_2)\overline{u} = \gamma'\phi_i(b) \\ \sum_j \phi_j(a_1)\overline{q}_j + \mathrm{j}\eta\omega\sum_j \phi_j(a_2)\overline{q}_j + \overline{u}(\omega^2 - \beta' - \mathrm{j}\eta\omega) = 0 \end{cases} \tag{23}$$

4. Chatter stability analysis

Stability of any machine–tool system can be shown in the diagrams in which the effects of width of cut, cutting velocity and other machining parameters on stability are analyzed. In these diagrams, the margins between stable and unstable conditions are shown with several lobes. The stability lobes are determined based on various conditions of both widths of cut and spindle speeds [1,2].

To analyze the chatter stability of the boring bar, the concept of mode summation is used to model the continuous boring bar as a set of sdof systems vibrating in individual modes of the beam. At each mode shape of the boring bar, the equation of motion in the feed direction without an absorber is given as

$$m\ddot{x} + c\dot{x} + kx = k_c w_c[x(t - T) - x(t)] \tag{24}$$

where all parameters are as defined in the previous section. Using the expressions

$$\omega_n = \sqrt{\frac{k}{m}}, \quad \zeta = \frac{c}{2\sqrt{km}}, \quad \Lambda = \frac{k_c w_c}{k}$$

yields the following equation:

$$\ddot{x}(t) + 2\zeta\omega_n\dot{x}(t) + \omega_n^2 x(t) = \Lambda\omega_n^2[x(t - T) - x(t)] \tag{25}$$

Transforming Eq. (25) into the Laplace domain results in

$$s^2 + 2\zeta\omega_n s + \omega_n^2 = \Lambda\omega_n^2(\mathrm{e}^{-sT} - 1) \tag{26}$$

The critical value of the width of cut at which the dynamic system switches from the stable condition to the unstable condition is determined as follows [1,2]:

$$w_{c,\mathrm{critical}} = -\frac{1}{2k_c G(\omega)} \tag{27}$$

where $G(\omega)$ is the real part of the transfer function of the dynamic system derived from Eq. (26) as follows:

$$\Gamma(s) = \frac{1}{s^2 + 2\zeta\omega_n s + \omega_n^2} \tag{28}$$

Substituting $s = \mathrm{j}\omega$ into Eq. (28), the real and imaginary parts of the transfer function are obtained as

$$\begin{aligned} G(\omega) &= \frac{\omega_n^2 - \omega^2}{R(\omega)} \\ H(\omega) &= \frac{-2\zeta\omega_n\omega}{R(\omega)} \\ R(\omega) &= (\omega_n^2 - \omega^2)^2 + (2\zeta\omega_n\omega)^2 \end{aligned} \tag{29}$$

Defining $\psi = \tan^{-1}[H(\mathrm{j}\omega)/G(\mathrm{j}\omega)]$ and after some mathematical manipulation [1,2], it can be shown that

$$T = \frac{1}{\omega}[2n\pi + \theta], \quad \theta = 3\pi + 2\psi \tag{30}$$

Using the set of Eqs. (27), (29) and (30), the stability lobe diagram of the dynamic model can be obtained [1,2]. For each mode shape of the cantilever beam model of the boring bar, the critical value of width of cut

and the stability lobe diagrams can be obtained. The overall critical width of cut may be obtained from the envelope of minimums of the lobe diagrams of the continuous system. At this critical value of width of cut, the dynamic system switches from the stable to the unstable condition.

5. Simulation, discussion and results

The boring bar is modeled as a cantilever Euler–Bernoulli beam. The parameters of the simulation are given in Table 1, which reflect a realistic boring case. The boring bar is a steel bar with a slenderness ratio (l/D) of 12.5. The boring bar mass is $m_i = 4.9\,\text{kg}$ and the cutting force amplitude is $F_c = 540\,\text{N}$. The feed rate of $f = 0.2\,\text{mm/rev}$, chip width of $w = 3\,\text{mm}$ and cutting coefficient of $k_c = 900\,\text{N/mm}^2$ are considered. To solve the coupled system of Eqs. (12) and (14) and to find the maximum deflection of the boring bar, the initial functional conditions for the first three modal coordinates are considered as $\overline{q}_1 = 0.1\,\text{mm}$, $\overline{q}_2 = \overline{q}_3 = 0$. Absorber parameters given in Table 1 are the initial values selected to start the simulation for obtaining the optimum values. The parameters are varied and their optimum values are determined. For the above input data, the first three natural frequencies of the boring bar with and without absorber are given in Table 2. It is observed that the two sets of natural frequencies are very close, but in general those of the system with the absorber are greater [26]. Furthermore, the three first mode shapes of the boring bar are shown in Fig. 7.

5.1. Optimizing the position of the absorber

To find the best position of the absorber, the beam is discretized into a finite number of elements. Then, the absorber is moved along the beam length by being placed at the end of successive elements and the deflection of the free end of the beam is computed for each case. Comparing these results, the minimum value of free-end deflection and the corresponding position of the absorber are determined.

It should be mentioned that this paper does not deal with chatter detection, but in the case of chatter, which was caused by the interaction of the tool (located on the boring bar) and the workpiece, chatter will be suppressed by designing an optimum vibration absorber. Since the boring bar is a continuous dynamic model, if its free-end deflection becomes minimized, the deflection of any points of the boring bar will be minimized too. So, minimizing the free-end deflection is an appropriate index that its satisfaction guarantees the chatter suppression.

The suppression of (non-chatter) forced vibration of the beam is studied by varying the stiffness of the absorber spring between 100 N/m and 5 kN/m. Then, the best position of the absorber for different values of spring stiffness is found. This procedure can be repeated for various excitation frequencies and various

Table 1
Realistic parameters of the vibration system

Boring bar specification		Absorber and cutting force specification	
Mass per unit length	$\rho = 9.8\,\text{kg/m}$	Mass	$m = 0.4\,\text{kg}$
Young modulus	$E = 180\,\text{GN/m}^2$	Spring stiffness	$k = 3000\,\text{N/m}$
Mass density	$\rho' = 7800\,\text{kg/m}^3$	Cutting force position	$b = 0.5\,\text{m}$
Diameter	$D = 4\,\text{cm}$	Forced frequency	$\omega = 600\,\text{rad/s}$
Length	$L = 50\,\text{cm}$	Number of modes	$n = 3$

Table 2
Natural frequencies of the boring bar

Natural frequencies of boring bar without absorber (rad/s)	Natural frequencies of boring bar with absorber (rad/s)
676	679
4232	4234
11,850	11,850

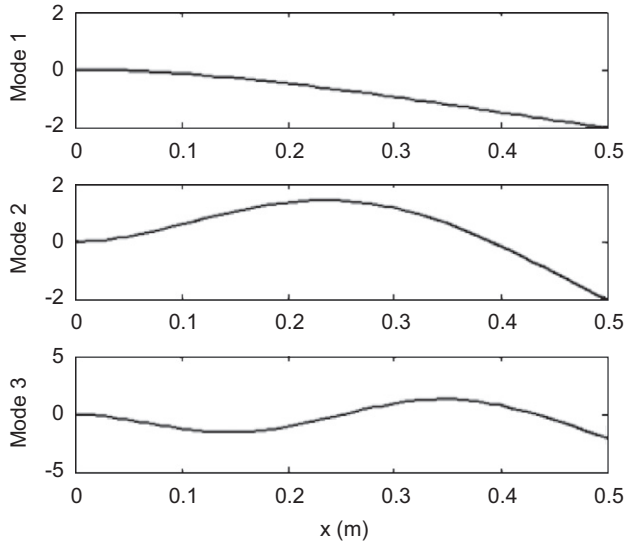

Fig. 7. The first three mode shapes of the boring bar.

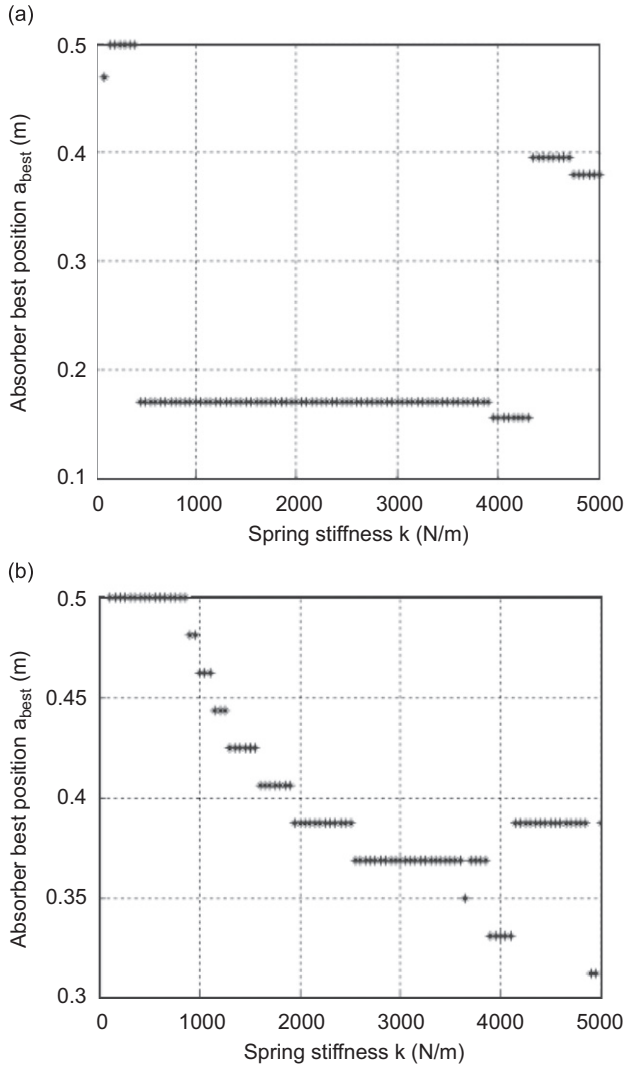

Fig. 8. Best position of absorber for different values of spring stiffness: (a) $\omega = 600\,\text{rad/s}$, $b = 0.5\,\text{m}$ and (b) $\omega_{n1} = 676\,\text{rad/s}$, $b = 0.5\,\text{m}$.

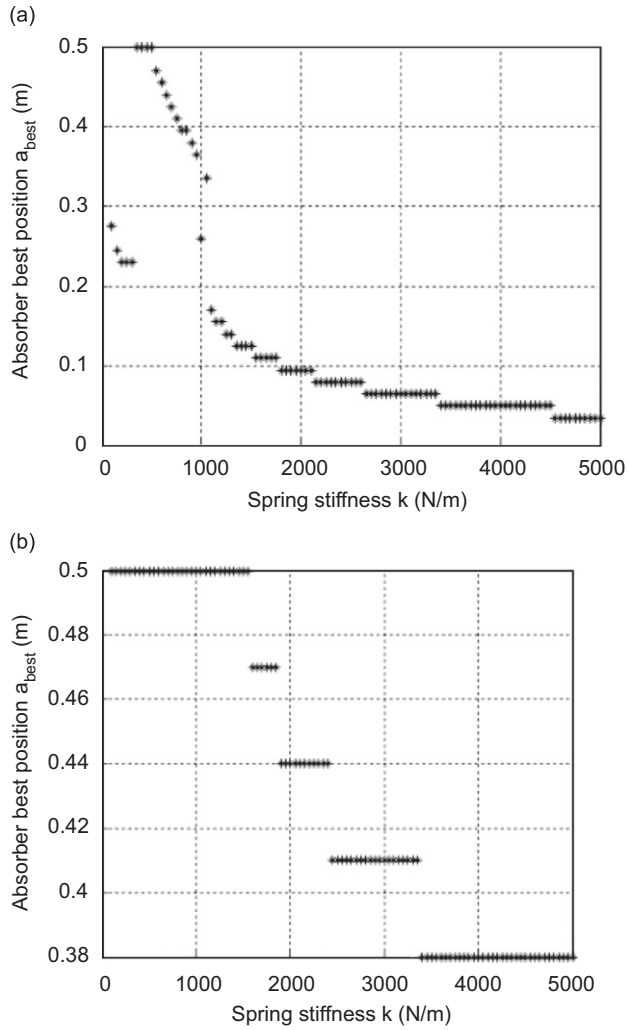

Fig. 9. Best position of absorber for different values of spring stiffness: (a) $\omega = 600\,\text{rad/s}$, $b = 0.4\,\text{m}$ and (b) $\omega_{n1} = 676\,\text{rad/s}$, $b = 0.4\,\text{m}$.

positions of the cutting tool. For example, Fig. 8 shows the best position of the absorber versus the spring stiffness at an arbitrary frequency ($\omega = 600\,\text{rad/s}$) and the first natural frequency ($\omega_{n1} = 676\,\text{rad/s}$) while the cutting tool is placed at the free end of the boring bar ($b = 0.5\,\text{m}$). Fig. 9 shows the case where the cutting tool is placed at $b = 0.4\,\text{m}$. Fig. 8a seems to be different from Figs. 8b and 9, because the dynamics of the boring bar is so sensitive to the interaction of parameters that a small variation of excitation frequency or cutting tool position can result in considerable change in the best position of the absorber.

5.2. Optimum design of the absorber and its effect on beam deflection

In order to design an effective absorber, the simulation is started with the initial values of absorber mass and stiffness as given in Table 1. It is assumed that the excitation frequency varies in the range of $400 < \omega < 4500\,\text{rad/s}$, which contains the first two natural frequencies of the boring bar. Using an algorithm developed in MATLAB, in each frequency, the best position of the absorber is found such that the free-end deflection of the boring bar is minimized.

The deflection curves of the beam at different excitation frequencies without/with the absorber are shown in Fig. 10, where resonance occurs at the first and the second natural frequencies of the boring bar. Theoretical values of deflection at the free end at these frequencies are $y_1 = 21$, $y_2 = 2\,\text{mm}$ for the system without the

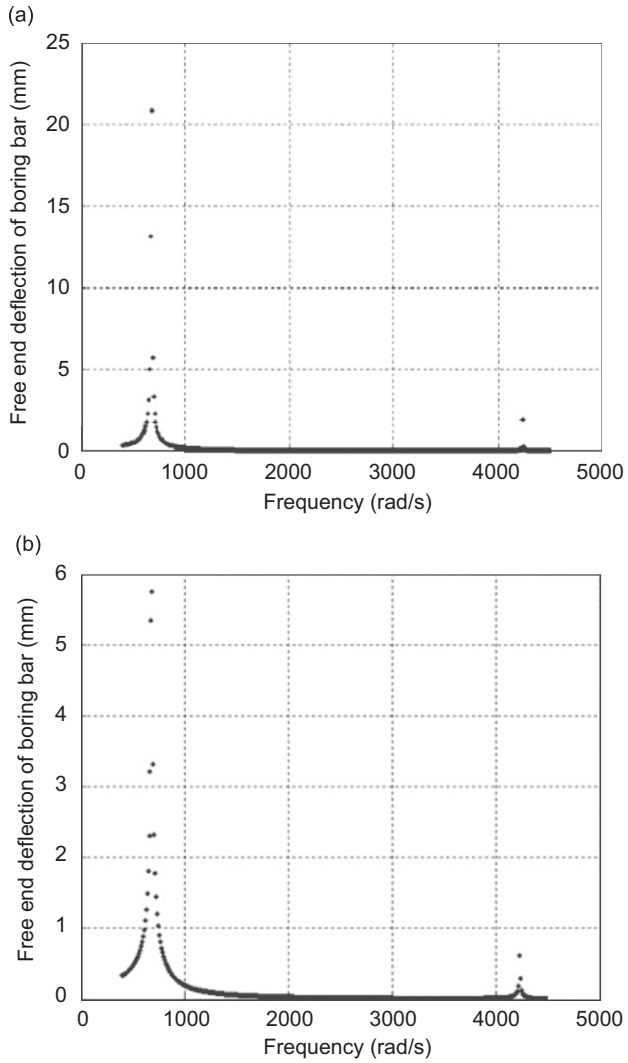

Fig. 10. Free-end deflection of the boring bar at different excitation frequencies: (a) without absorber and (b) with absorber.

absorber, but are reduced to $y_1' = 5.8$, $y_2' = 0.6$ mm after using the absorber. However, this absorber is not the optimum one.

To design an optimum absorber, the mass of the absorber is assumed to be constant ($m = 0.4$ kg). Keeping the other parameters at the values given in Table 1, three regions are considered for spring stiffness. In each region, using an algorithm that varies both values of spring stiffness and its position, the best values of these parameters that result in a minimum value of free-end deflection are found. For the boring bar with specifications given in Table 1 and with the excitation frequency of $\omega = 600$ rad/s, the best value of stiffness and the absorber position are found as $k = 3400$ N/m and $a_{\text{best}} = 0.44$ m, respectively. For the other frequencies, the optimum absorber is determined similarly, e.g., at the first natural frequency of the boring bar, the results of Table 3 are achieved. The best values of stiffness and absorber position are $k = 4200$ N/m and $a_{\text{best}} = 0.36$ m, respectively.

In two arbitrary values of frequency, a non-natural frequency, e.g., $\omega = 600$ rad/s, and the natural frequency $\omega = 676$ rad/s, the optimum values of absorber parameters are found as shown in Table 4. For example, deflection curves of the boring bar at its first natural frequency, without/with the optimum absorber (with specification given in Table 4), are shown in Fig. 11. Free-end deflections without/with the absorber are

Table 3
Best values of spring stiffness and absorber position at $\omega_{nl} = 676\,\text{rad/s}$

k (kN/m)	Best value of k	Best position of absorber	Boring bar midpoint deflection (mm)
$0.01 < k < 0.1$	0.1	0.42	2.5
$0.1 < k < 1$	0.95	0.5	1.4
$1 < k < 5$	4.2	0.36	0.18

Table 4
Optimum values of the absorber parameters

	Absorber mass (constant) (kg)	Optimum spring stiffness (N/m)	Best position of absorber (m)
$\omega = 600\,\text{rad/s}$	$m = 0.4$	$k = 3400$	$a_{\text{best}} = 0.44$
$\omega = 676\,\text{rad/s}$	$m = 0.4$	$k = 4200$	$a_{\text{best}} = 0.36$

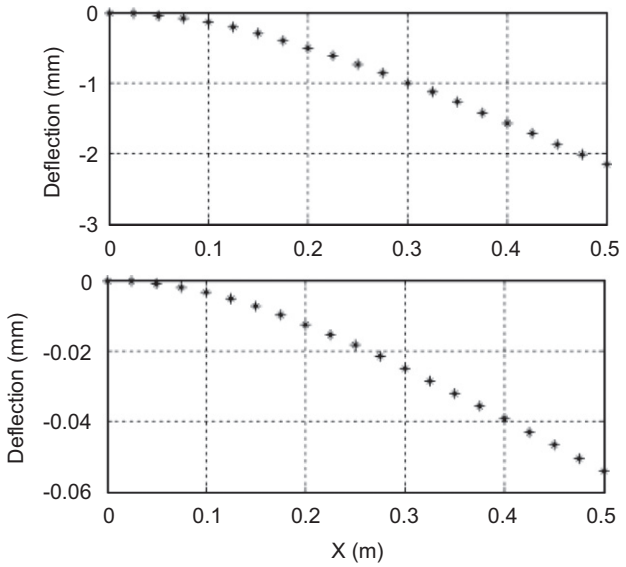

Fig. 11. Deflection curves of the boring bar: (a) without absorber and (b) with optimum absorber.

$y_0 = 2.2\,\text{mm}$ and $y = 0.055\,\text{mm}$, respectively. The deflection of the free-end point is reduced to about 1/40 of the original value.

5.3. Stability analysis

In this section, the stability of the boring bar is analyzed separately in its first three mode shapes. At the natural frequencies given in Table 1, Eqs. (27), (29) and (30) are applied and the stability lobe diagrams at the corresponding mode shape of the boring bar are found (Section 4). Fig. 12 shows the stability lobes diagram of this model. Sets of curves I, II and III of this figure represent the stability lobe diagram at chatter frequencies around the first, second and third mode of the boring bar. According to this figure, at higher modes, larger critical widths of cut are obtained.

Let us consider the stability lobe diagram I. At a given spindle speed, e.g., at $N = 900\,\text{rpm}$, point A represents the stable condition while point B represents the unstable condition. For the boring process with the

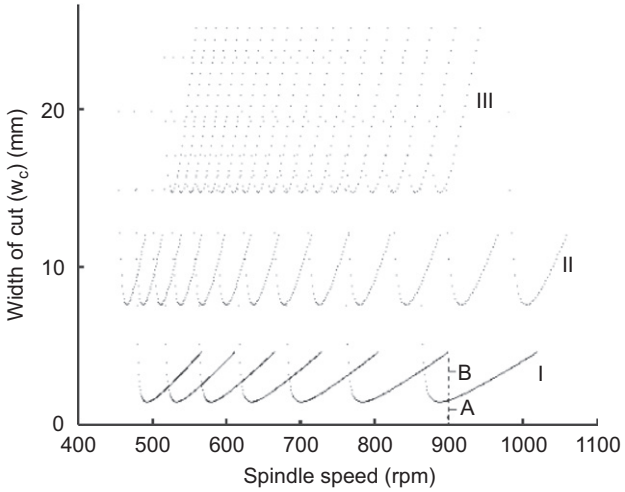

Fig. 12. Stability lobes diagram for the first mode I, second mode II and third mode III. For mode I: point A is stable and point B is unstable.

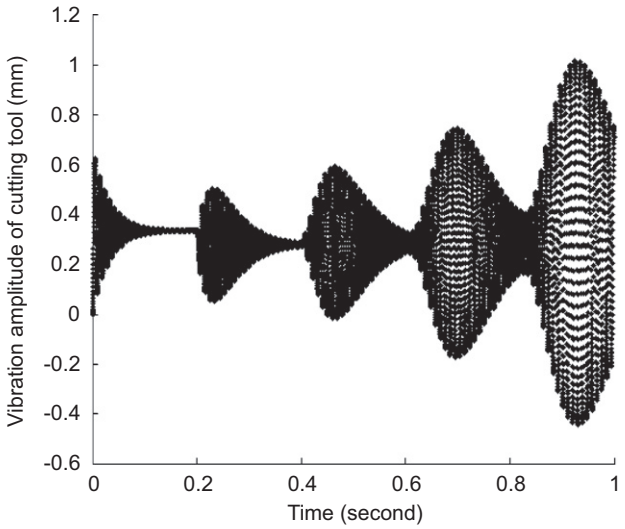

Fig. 13. Time response of the system in unstable condition before the absorber is applied.

conditions of point B in which spindle speed is $N = 900$ rpm and width of cut is $w_c = 3$ mm, an unstable time response is expected as shown in Fig. 13.

Next, an absorber with parameters given in Table 3 is used to suppress chatter. Fig. 14 shows the time response of the system after using the absorber. It is observed that the absorber reduces the absolute value of the real part of transfer function of the dynamic system. Therefore, according to Eq. (27), using the absorber at a given spindle speed, the critical width of cut is increased significantly. Consequently, according to Fig. 12, higher values of width of cut can be achieved without reaching an unstable condition (from stable point A to unstable point B in Fig. 12). In this way, higher MRR can be achieved after applying the optimum absorber.

6. Conclusions

In this paper, the optimum design of a tuneable vibration absorber (TVA) is presented and applied to suppress chatter in boring manufacturing process. The formulation is done for an absorber composed of mass,

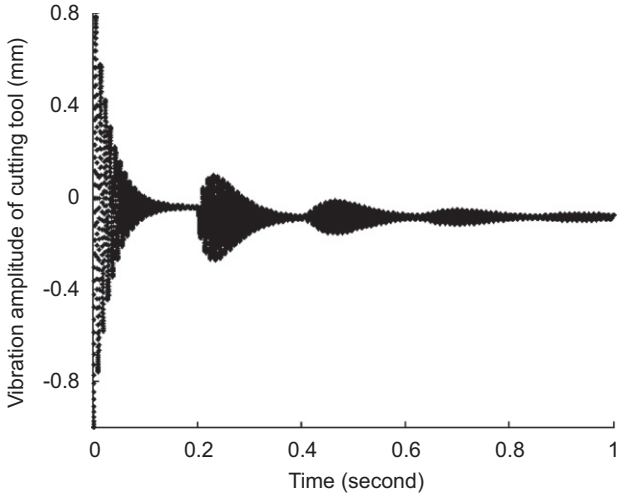

Fig. 14. Time response of the system in unstable condition after applying the optimum absorber.

spring and dashpot elements. To have a more accurate model, the effect of spring mass is considered too. The boring bar is modeled as a cantilever Euler–Bernoulli beam. The optimum specifications of the absorber such as spring stiffness, absorber mass and its position are determined by developing an algorithm based on the mode summation method. By considering all parameters to be constant and changing one parameter or two parameters simultaneously, such as absorber position and spring stiffness, the optimum specifications of the absorber are determined. It is shown that the best position of the absorber to minimize free-end deflection of the beam, and consequently all other points, depends on both chatter frequency and cutting force position. Results show that the optimum absorber acts effectively, especially in the resonance condition. After studying the forced vibration, chatter stability is analyzed for the boring bar. The stability lobes diagrams, which indicate the critical value of width of cut, are found in the first three mode shapes of the boring bar. Results show that at higher modes larger critical width of cut and consequently more material removal rate (MRR) can be achieved.

In the case of self-excited vibration, which is caused by selection of a large width of cut and associated with a delay differential equation, the dynamic model is simulated using SIMULINK Toolbox of MATLAB. Similar procedure to that of the force vibration case is followed to design the optimum absorber under chattering conditions. The optimum absorber suppresses the chatter and increases the limit of stability. Therefore, a higher MRR can be obtained at a given spindle speed without reaching unstable conditions. Finally, the effect of spring mass is included in this model. Among various variables such as spring stiffness, absorber mass and machining parameters, the dynamic system only may be sensitive to the resonance condition (near the chattering). Even at this condition, the absorber works effectively and the optimum design is almost robust to the possible uncertainties. Since the TVA including damping may be useful in other applications with more precise assumptions, the formulation has been developed and presented for future works.

References

[1] H.E. Merrit, Theory of self-excited machine–tool chatter: contribution to machine–tool chatter research—1, *Transactions of ASME—Journal of Engineering for Industry B* 87 (4) (1965) 447–454.
[2] S.A. Tobias, W. Fishwick, The chatter of lathe tools under orthogonal cutting conditions, *Transactions of the American Society of Mechanical Engineers* 80 (1958) 1079.
[3] F. Koeinsberger, J. Tlusty, *Machine Tool Structures*, Vol. 1, Pergamon Press, New Jersey, 1970.
[4] J. Tlusty, F. Ismail, Basic nonlinearity in machining chatter, *C.I.R.P. Annual* 30 (2) (1981) 229–304.
[5] R.N. Arnold, The mechanism of tool vibration in the cutting of steel, *Proceedings of the Institution of Mechanical Engineers* 154 (1946) 261.
[6] H. Nayfeh, D. Mook, *Nonlinear Oscillations*, Wiley Interscience, New York, 1979.

[7] N. Hanna, S.A. Tobias, A theory of nonlinear regenerative chatter, *ASME Journal of Engineering in Industry* 96 (1974) 247.
[8] N. Deshpande, S. Fofana, Nonlinear regenerative chatter in turning, *Journal of Computer Integrated Manufacture* 17 (2001) 107–112.
[9] G. Stepan, T. Insperger, R. Szalai, Delay, parametric excitation, and the nonlinear dynamics of cutting process, *Journal of Bifurcation and Chaos* 15 (9) (2005) 2783–2798.
[10] Y.S. Tarng, J.Y. Kao, E.C. Lee, Chatter suppressions in turning operations with a tuned vibration absorber, *Journal of Materials Processing Technology* 105 (2000) 55–60.
[11] E.C. Lee, C.Y. Nian, Y.S. Tarng, Design a dynamic vibration absorber against vibrations in turning operations, *Journal of Materials Processing Technology* 108 (2001) 278–285.
[12] N.D. Sims, Vibration absorbers for chatter suppression: a new analytical tuning methodology, *Journal of Sound and Vibration* 301 (2000) 592–607.
[13] S.G. Tewani, K.E. Rouch, B.L. Walcott, A study of cutting process stability of a boring bar with active dynamic absorber, *International Journal of Machine Tools & Manufacture* 35 (1) (1995) 91–108.
[14] J.R. Pratt, A.H. Nayfeh, Active vibration control for chatter suppression, AIAA-97-1210, 1997, pp. 623–633.
[15] J.R. Pratt, A.H. Nayfeh, Chatter control and stability analysis of a cantilever boring bar under regenerative cutting conditions, *Philosophical Transactions of the Royal Society of London, part A* 359 (2001) 759–792.
[16] S. Ema, E. Marui, Suppression of chatter vibration of boring tools using impact dampers, *International Journal of Machine Tools & Manufacture* 40 (2000) 1141–1156.
[17] N.D. Sims, A. Amarasinghe, K. Ridgway, Particle dampers for workpiece chatter mitigation, *ASME International Mechanical Engineering Congress and Exposition*, Orlando, FL, USA, November 5–11, 2005 (IMECE2005-82687).
[18] S. Smith, T. Delio, Sensor-based chatter detection and avoidance by spindle speed selection, *ASME Journal of Engineering for Industry* 114 (1992) 486–492.
[19] S. Smith, J. Tlusty, Stabilizing chatter by automatic spindle speed regulation, *C.I.R.P. Annual* 41 (1) (1992) 433–436.
[20] Y.S. Liao, Y.C. Young, A new online spindle speed regulation strategy for chatter control, *International Journal of Machine Tools & Manufacture* 36 (5) (1996) 651–660.
[21] C. Mei, Active regenerative chatter suppression during boring manufacturing process, *Journal of Robotics & Computer Integrated Manufacturing* 21 (2005) 153–158.
[22] M. Shiraishi, K. Yamanaka, H. Fujita, Optimal control of chatter in turning, *Journal of Machine Tools & Manufacture* 31 (1) (1991) 31–43.
[23] L. Hakansson, I. Claesson, P.O. Sturesson, T.L. Lago, Active control of chatter in turning, *IMAC-XVII, International Modal Analysis Conference*, 1999, pp. 1799–1805.
[24] F. Bakhtiari-Nejad, H. Moradi, Optimum design of vibration absorber with variable position for an Euler–Bernoulli beam under moving point excitation, *14th International Congress of Sound & Vibration ICSV14*, Cairns, Australia, 2007.
[25] E.P. Degarmo, T. Black, R.A. Kohser, *Materials and Processes in Manufacturing*, ninth ed., Wiley, NY, 2003.
[26] D.J. Inman, *Engineering Vibration*, Prentice-Hall International Inc., Englewood, NJ, 1994.